A catalyst-free process for gas ozonation of reduced sulfur compounds

Leticia Vitola Pasetto, Valérie Simon, Romain Richard, Jean-Stéphane Pic, Frédéric Violleau, Marie-Hélène Manero

Version of Record: https://www.sciencedirect.com/science/article/pii/S1385894719328293
Manuscript_4724adaae55d2e45f6dba300811b6318

A catalyst-free process for gas ozonation of reduced sulfur compounds

Leticia Vitola Pasetto[1,2], Valérie Simon[2], Romain Richard[1], Jean-Stéphane Pic[3], Frédéric Violleau[2], Marie-Hélène Manero[1]*

(1) Laboratoire de Génie Chimique, Université de Toulouse, CNRS, INPT, UPS, Toulouse, France.
(2) Laboratoire de Chimie Agro-industrielle, LCA, Université de Toulouse, INRA, Toulouse, France.
(3) TBI, Université de Toulouse, CNRS, INRA, INSA, Toulouse, France.

Abstract (maximum 250 words)

The feasibility of homogenous gas ozonation process was investigated in order to reduce the negative environmental impact caused by reduced sulfur compounds (RSCs). Emitted from a variety of industrial plants, this class of compounds are known by their odor properties. Selecting hydrogen sulfide (H_2S), methyl ethyl sulfide (MES) and dimethyl disulfide (DMDS) as representative odorous RSCs, the influence of four gas ozonation process parameters (ozone concentration, humidity level, reactor temperature and residence time) on their removal efficiencies was evaluated using a Doehlert experimental design in an experimental domain compatible with industrial constraints. Ozone concentration was the only process parameter that has resulted in a positive – but limited – effect on the removal efficiency of the mix of RSCs. However, even if ozone was present in large excess (20 times the RSCs concentration), MES and DMDS were slightly consumed (around 30%). Only H_2S has shown interesting removal efficiencies (up to 80%). In addition to the measurement of reagent concentrations, Selected Ion Flow Tube coupled with Mass Spectrometry (SIFT/MS) was applied to identify and quantify the potential products of RSCs-ozone reaction. Methyl ethyl sulfone ($MESO_2$) was found to be the primary product of MES, whereas methyl methanethiosulfinate (DMSOS) and sulfur dioxide (SO_2) for DMDS, suggesting that the organic monosulfide and disulfides would not follow the same reaction mechanism with ozone in gas phase. In addition, SO_2 and H_2O may not be the only end products for H_2S ozonation, since additional peaks were detected in SIFT/MS spectra.

*Corresponding author. Email: marie-helene.manero@iut-tlse3.fr . Tel. +33 5 62 25 89 23. Current address: Université de Toulouse / IUT GCGP, Laboratoire de Génie Chimique 4 Allée Emile Monso, BP84234, 31 432 Toulouse Cedex 4, France.

Keywords (maximum 6)

Odor compounds, ozone, SIFT/MS, Doehlert design, gas treatment, homogenous ozonation

1. Introduction

Usually associated to odor nuisance and to potential health effect, reduced sulfur compounds (RSCs) are one of major concern in air pollution [1,2]. Defined by the presence of sulfur in a reduced state (oxidation number at -2 and -1), RSCs are composed by several classes of organosulfur compounds – such as mercaptans (thiols), sulfides and disulfides – which are usually characterized by their strong odor even at low concentrations (at ppbv level) [1]. In addition, they are air pollutants found in a variety of emission sources known as odor sensitive sites, such as pulp-and-paper and fertilizer industrial plants, wastewater treatment, agriculture, pig production and livestock facilities [1,3,4].

In an industrial context, the reduction of the negative impact caused by odor compounds is mostly performed by wet scrubbers, regenerative thermal oxidation and biofiltration [4–8], by which RSCs are converted to oxides, sulfoxides or sulfones that are expected to present higher values of odor threshold limits (ODT) [4]. Even if high removal efficiencies can be achieved from these classical techniques, some drawbacks still remain, such as high operating temperatures, high chemicals demand and low flexibility regarding the operating conditions [4,5,9]. In addition, biofilter devices have shown low removal efficiency for some examples of RSCs, in particular dimethyl sulfide (DMS) and dimethyl disulfide (DMDS) [5,9]. Oxidative gas treatments based on photolysis, catalysis or photocatalysis and homogenous ozonation techniques have emerged as potential alternatives to this context [4,9–13]. In this study, we were especially interested in a catalyst-free homogenous ozonation technique, since it requires a simpler set-up configuration, operation at ambient or reduced temperature and it has been successfully applied at the industrial scale for controlling nitrogen oxides [14–17]. In the case of RSCs, only few studies were focused on ozone oxidation treatment, even though, interesting results have been reported for the ozonation of hydrogen sulfide (H_2S), methyl mercaptan, DMS and DMDS [10,17,18].

The investigation of RSCs-ozone gas phase reaction has been mainly conducted in order to understand phenomena in lower and upper atmospheres, involving operating conditions distinct from those applied in an industrial gas treatment [19–21]. In the case of H_2S, contradictory values were found for the reaction rate constant with ozone in the gas phase, varying by 4 orders of magnitude (from 1×10^{-20} cm^3 $molecule^{-1}$ s^{-1} [20,22–24] to 6×10^{-16} cm^3 $molecule^{-1}$ s^{-1} [21,25]), which may be the consequence of the different experimental techniques and operating conditions applied in these studies (simulating tropospheric or stratospheric conditions, for example). The reaction mechanism proposed for H_2S-O_3 reaction has also been a subject of disagreement: Hales *et al* [26] have suggested that sulfur dioxide (SO_2) and H_2O were the main products whereas Glavas and Toby [25] have found that oxygen (O_2) was the most abundant product in comparison with SO_2, H_2O and H_2S (produced from the $SH^\bullet$ + $SH^\bullet$ reaction). More recent studies based on molecular modelling have concluded that SO_2 + H_2O generation was the most thermodynamically important pathway (with the most negative value of Gibbs free energy) at temperatures up to 730 °C, whereas at higher temperatures, O_2, thioperoxol (HSOH) and radicals, such as $HOSO^\bullet$, $SH^\bullet$, $HO_3^\bullet$ and $OH^\bullet$ become also important [23,24]. In the case of sulfur-containing organic compounds, the rate constants of gas phase reaction with ozone are expected to be about 10^{-19} to 10^{-20} cm^3 $molecule^{-1}$ s^{-1}, considered as a slow reaction in atmosphere [27,28]. Concerning the reactional mechanism between sulfur-containing organics and ozone, most of studies have been focused on reactions in the liquid phase, in which sulfides are firstly oxidized to sulfoxides and then to sulfones. In an analogous way, disulfides are oxidized to thiosulfinate, thiosulfonate or disulfoxide, and then to disulfone [27,29–31]. The generation of sulfonic anhydride was reported by Barnard [30] and by Douglass [31]. The only few studies that have investigated the reaction between sulfides and ozone in the gas phase were carried out at low pressure conditions (~1 kPa) [32,33]. Martinez and Herron [32] suggested a different mechanism from the sequential oxidation reported in the liquid phase, in which O_3 attack on DMS would follow a chain reaction that involves carbon-sulfur bond scission, generating SO_2 as one of by-products. In their studies of gas reaction between ozone and several RSCs (H_2S, methyl mercaptan, DMS and DMDS) in a beam-gas apparatus, Glinski and Dixon [33] have reported the generation of SO_2 (evidenced by chemiluminescence from electronically excited SO_2). In a more recent study, Kastner *et al* [4] have also reported SO_2 as one

primary product for catalytic gas ozonation of H_2S and methyl mercaptan at room conditions, whereas dimethyl sulfoxide (DMSO) and dimethyl sulfone ($DMSO_2$) were identified as primary products of DMS oxidation.

In this work, the feasibility of RSCs homogenous gas ozonation as an odor treatment process was investigated in an industrial emission context, characterized by a short residence time (up to a few seconds [9]) and a complex gas mixture [34–36]. The influence of four process parameters (ozone concentration, humidity level, reactor temperature and residence time) on the removal efficiency of a multipollutant gas stream by ozone oxidation was evaluated using a Doehlert experimental design. Selecting H_2S, methyl ethyl sulfide (MES) and dimethyl disulfide (DMDS) as representative RSCs, their primary products were investigated, thanks to the use of selected ion flow tube mass spectrometry (SIFT/MS) as the online analytical device.

2. Materials and methods

2.1. Chemicals

H_2S, MES and DMDS have been selected as the representative RSCs due to their low ODT (0.1 ppbv for H_2S, 7 ppbv for MES and 0.3 ppbv for DMDS [34]). In addition, each compound represents a class of RSCs: inorganic sulfide, organic (mono)sulfide and organic disulfide, respectively. Primary standards contained in a single gas cylinder were purchased from Air Liquide, France (Crystal® gas mixture designed on request, containing 80 ppmv of H_2S; 300 ppmv of MES and 800 ppmv of DMDS in 99.88% molar of N_2 with uncertainty at 25%).

2.2. Ozonation set-up

The gas phase reaction was performed in a continuous flow, using a jacketed glass tubular reactor (250 mL) (Figure 1). The reactor was kept at atmospheric pressure during all experiments (101.3 kPa). The gas temperature at the reactor inlet and outlet were constantly monitored (PT100 temperature sensors).

Dry air (oil-free air ISO 8573-1 class 0, dew point equal to -40 °C at 101.3 kPa) generated by an air compressor (ZR55, Atlas Copco France) equipped with an air filter (Olympian Plus, Norgren, UK) was fed to a humidification system (Serv'Instrumentation, France), in which the moisture

level was controlled by a humidity and temperature transmitter (HMT333, Vaisala, Finland). The RSCs multipollutant mixture from the gas cylinder was injected into the dilution air stream before the reactor inlet, which gas flows were controlled by mass flowmeters (SLA 5850S-B Brooks Instruments, USA). Ozone was generated by a plasma discharge ozone generator (HTU500 AZCO Industries Limited, Canada) fed with oxygen (99.999%, Linde Gas, France). Depending on the power regulator of the ozone generator, ozone concentration could vary from 2300 ppmv to 4800 ppmv (for a fixed inlet oxygen flow of 500 NmL min^{-1} in the ozone generator). Before feeding the reactor, the ozone-oxygen stream was controlled by a mass flowmeter (SLA 5850S-B Brooks Instruments, USA).

In order to study the reaction at higher temperatures (up to 60 °C), the dilution air stream was sent to a heating stage, composed by a stainless steel smooth-coil immersed in a synthetic thermoliquid bath (Ultra 350, Lauda, Germany). In addition, the reactor was heated (from 20 °C to 60 °C) using the synthetic thermoliquid with a heated circulating oil bath (Model 1160S, VWR, USA). All gas lines (from the humidification system until the analytical device) were isolated and heated to prevent condensation inside the PTFE lines (orange hatched area in Figure 1).

Ozone concentrations were measured by an UV analyzer (BMT 964, BMT MESSTECHNIK GMBH, Germany) directly after its production and also by SIFT/MS (Voice 200*ultra*, Syft Technologies Ltd, New Zealand) at the reactor outlet. The RSCs concentrations were measured by SIFT/MS installed directly at the reactor outlet in an online system. Therefore, the inlet RSCs concentrations ($[RSCs]_{in}$) were measured without any presence of ozone whereas the outlet RSCs concentrations ($[RSCs]_{out}$) were measured in the presence of ozone.

2.3. SIFT/MS analysis

In SIFT/MS, the quantification of an analyte (neutral compound) is based on the soft ionization reaction of the analyte with a precursor ion in a region with fixed conditions (called flow tube), generating product ions at a specific mass-to-charge ratio (*m/z*), which are quantified by a quadrupole mass spectrometer. A range of positive ions (H_3O^+, NO^+, O_2^+) is available for the quantification of most organic compounds and five negative ions (NO_2^-, NO_3^-, O_2^-, HO^-, O^-) for the quantification of compounds that are not ionized by the positive ions, such as ozone, SO_2 and SO_3.

The principle of the SIFT/MS device has been deeper explained previously [37]. In a summarized form, the analyte concentration ($[A]_{sample}$ in ppmv) is calculated by Equation 1 involving the rate coefficient (k_I in cm^3 $molecule^{-1}$ s^{-1}) of the reaction between the neutral compound and the precursor ion and the ratio between product ion count rate (P in cps) and precursor ion count rate (I in cps) [38]. The factor γ depends on the operating conditions of the flow tube, reaction time and on the carrier gas and sample flows [38], which was around 1.4×10^{-7} s molecule cm^{-3} during the experiments. The required parameters for quantification of the four reagents (H_2S, MES, DMDS and O_3) by SIFT/MS are shown in Table 1. The limit of detection (LOD) obtained by SIFT/MS was 20 pptv for H_2S, 60 pptv for MES, 200 pptv for DMDS and 45 ppbv for O_3 (based on the expression reported in Francis *et al*, 2009 [39] and a measurement time of 100 s).

$$[A]_{sample} = \frac{P}{I}\frac{\gamma}{k_I} \quad (1)$$

2.4. Doehlert experimental design

Besides the common advantages of a multivariate experimental design (such as process optimization and evaluation of the most impacting parameters and their positive or negative interaction), a Doehlert design has been chosen for its high efficiency (experimental design with the fewest number of experiments needed). It can easily optimize the system and describe a non-linear interaction because of its second-order fitting model; it is also an adaptable design, due to the possibility of moving through the experimental domain.

Aiming a better understanding of the process, three different operating conditions have been studied as factors: (1) humidity level expressed in water concentration ($[H_2O]$), (2) inlet ozone concentration ($[O_3]_{in}$) and (3) reactor temperature ($T_{reactor}$). The effect of the residence time in the reactor (t_{RES}) on removal efficiencies of RSCs was not included as a factor on the Doehlert experimental design, after running preliminary tests. The range for each parameter (Table 2) was chosen to approach the industrial conditions with a determined inlet RSCs concentration : 0.46 ± 0.08 ppmv H_2S; 1.8 ± 0.2 ppmv MES and 4.0 ± 0.4 ppmv DMDS. In most of the experiments, ozone was in excess compared to the sum of $[H_2S]_{in}$, $[MES]_{in}$ and $[DMDS]_{in}$ (expressed as $[RSCs]_{in}$), except when $[O_3]_{in}$ was at 5 ppmv.

The fitting model proposed by Doehlert is a second order equation, using four coefficients: a_0 (constant term that corresponds to the response at the center of the domain); a_n (linear terms); a_{nm} (interaction terms) and a_{nn} (quadratic terms). The model is described by Equation 2. The higher the value of a_n, the stronger the influence in the response (Y_i), where i refers to the specific RSCs (H_2S, MES or DMDS). The a_{nm} express interaction between two variables, that could be positive (synergy) or negative. The a_{nn} reveal the geometry of the response surface [40]. The X_n represent the coded variables and are calculated by Equation 3, where U_n is the real value of the variable; $U_{n\ center}$ is the value at the center point (it is the average between the maximum and the minimum of variable range), ΔU_n is the variation between maximum value of the U_n range and the U_{n0}; β_n is the maximum value of the coded variable in Doehlert table (Table SI-1, Support Information), equal to 1.0 for n = 1; 0.866 for n = 2; 0.816 for n = 3. Y_i^{exp} is the efficiency removal of specific RSCs and calculated by Equation 4. The Doehlert coded values for three-factor design are in Table SI-1, Support Information. In order to verify the repeatability, the experiment at the center of the experimental domain ($X_1 = X_2 = X_3 = 0$) was run in quadruplicate.

$$Y_i = a_0 + \sum_{n=1}^{3} a_n X_n + \sum_{n=1}^{3} a_{n\,n} X_n^2 + \sum_{n=1}^{3} \sum_{m=n+1}^{3} a_{n\,m} X_n X_m \quad (2)$$

$$X_n = \left[\frac{U_n - U_n^{center}}{U_n^{max} - U_n^{center}}\right] \beta_n \quad (3)$$

$$Y_i^{exp} = \frac{[i]_{in} - [i]_{out}}{[i]_{in}} \text{ with } i = H_2S, \text{MES and DMDS} \quad (4)$$

Analysis of variance (ANOVA) was employed to calculate and to test the statistical significance of each coefficient (a_0, a_n, a_{nm}, a_{nn}) into Y_i using Minitab® (version 18.1). In this study, the coefficient values were obtained considering a confidence interval equal to 95%. Fitting models and coefficients were considered statistically significant when their P-values were inferior to 0.005. The statistical significance is related to null hypothesis (variations in Y_i are not correlated to variations in X_n, *i. e.*, $X_n = 0$). Thereby, the smaller P-value, the less likely the null hypothesis, which means the correlation between the factors and Y_i is more probable.

3. Results and discussion

3.1. Effect of residence time

Preliminarily tests of catalyst-free ozonation of H_2S, MES and DMDS were carried out in order to verify the effect of increasing t_{RES} in the removal efficiency of RSCs (Figure 2). The respective uncertainties were calculated by the method of propagation of error, considering the uncertainty of the air polluted generation system (estimated < 5%) and the uncertainty from the SIFT/MS quantification (obtained from LabSyft® Data Analysis and equal to the standard deviation of the mean concentration for a measurement time of 500 s).

With $T_{reactor}$ at room conditions (equal to 20 °C) and at the highest ozone inlet concentration ($[O_3]_{in}$ = 100 ppmv), H_2S has presented the higher removal efficiency, above 80%, whereas the highest level for the removal efficiencies of MES and DMDS were about 40% and less than 20%, respectively, despite the large excess of ozone ($[O_3]_{in}/[RSCs]_{in}$ equal to ~20). The increase of t_{RES} (from 2 to 20 s) has not resulted in a considerable improvement on the removal efficiency of H_2S and DMDS. Only MES has shown a potential positive impact of t_{RES}, since the removal efficiency has increased from 27 ± 5% to 45 ± 11%. However, the enhancement of the removal efficiency was hidden by the increase of the uncertainty of the system (due to the use of the gas flows in their lowest values). In comparison with the studies of Tuggle [18], none of RSCs investigated (H_2S, DMS and DMDS) have presented a significant increase of the removal efficiency when the residence time was increased from 10 to 60 s. This is in agreement with Zhang and Pagilla [10] who have observed that the increase of t_{RES} from 8 to 40 s have not considerably enhanced the removal efficiency of H_2S.

3.2. Effect of ozone concentration, reactor temperature and humidity level

The experimental removal efficiency of H_2S, MES and DMDS obtained by applying Doehlert design are presented in Figure 3 for a fixed 2 s residence time (as the t_{RES} has shown a negligible effect). H_2S has achieved similar removal efficiency value compared to the preliminary tests – above 80% – when $[O_3]_{in}$ was at least 50 ppmv. The highest level for the removal efficiencies of

MES and DMDS were about 30%, obtained when ozone was in large excess compared to $[RSCs]_{in}$ (close to 20 times with $[O_3]_{in}$ at 100 ppmv).

The analysis of variance (Table 3) was performed for the removal efficiency of each RSCs separately, resulting in acceptable precision ($R^2 > 0.95$) and significant correlations between one or more factors with the removal efficiencies (P-value < 0.005) for all three models.

The P-value of the linear, quadratic and interaction terms coefficients proposed by Doehlert are also shown in Table 3. None of those related to $[H_2O]$ (factor n = 1) for all three RSCs have shown P-value < 0.005, which indicates that the removal efficiency of all RSCs by ozone was not affected by the humidity level for the operating conditions tested. The lack of influence even in high humidity levels suggests that the expected hydroxyl radicals generation ($HO^{\bullet}$) from the decomposition of O_3 with H_2O in gas phase [10,14] do not interfere on the ozonation of RSCs for the operating conditions applied in this study, which could imply that the oxidation reaction mainly happens *via* molecular attack of ozone on the RSCs.

$[O_3]_{in}$ (factor n = 2) was the only factor which the linear term has presented P-value = 0 for all RSCs. For the case of MES and H_2S, the quadratic term was also significant, which means that the correlation between the $[O_3]_{in}$ and removal efficiencies are not linear, showing a slowdown in case of MES (Figure 3B) and a parabola curve for the case of H_2S (Figure 3A). As it is evidenced in Figure 4, the coefficient a_2 (linear term of $[O_3]_{in}$) was positive and presented the highest values regarding the others terms (except a_0) for all three RSCs.

The effect of $T_{reactor}$ (factor n = 3) was negligible for the removal of MES (P-value > 0.005). This is shown in Figure 3B, in which experiments carried out with $T_{reactor}$ at 20 °C, 40 °C and 60 °C have given similar behavior as function of ozone concentration. In case of DMDS, $T_{reactor}$ has presented a positive effect (positive value of a_3 on Figure 4) and non-linear correlation (P-value of a_3 and a_{33} < 0.005). As we can see on Figure 3C, the effect of the temperature on removal efficiency of DMDS by ozone oxidation was visible from 20 °C (for $[O_3]_{in}$ at 100 ppmv, DMDS was 9 ± 5% removed) to 40 °C (for $[O_3]_{in}$ at 100 ppmv, DMDS was 30 ± 5% removed), but less notable from 40 °C to 60 °C (for $[O_3]_{in}$ at 100 ppmv, DMDS was 30 ± 4% removed). This lack of proportionality on $T_{reactor}$ could be explained by the low values of removal efficiency of DMDS,

which in association with a considerable variability of the system have hidden the positive effect for the range at higher temperatures. Low removal values and high variability could also explained the poor fitting of the model for removal efficiency of DMDS at $T_{reactor}$ = 20 °C (shown in Figure 3C). In case of H_2S, a surprising negative effect of the $T_{reactor}$ on the removal efficiency was evidenced: P-value of a_3 equal to 0 in Table 3 and the negative value of a_3 in Figure 4.

The negative effect of temperature on the H_2S removal and the parabolic behavior of H_2S removal as function of ozone concentration could suggest a kinetic equilibrium in place. However, we have concluded that these phenomena were a consequence of analytical artifacts in SIFT/MS due to water interference on H_2S quantification [37]. Because of a decrease on the count rate of the characteristic product of H_2S as function of the water vapor in the sample, the relative uncertainty related to H_2S quantification by SIFT/MS has varied, which resulted that the uncertainty of measuring 0.5 ppmv of H_2S in presence of 40000 ppmv of H_2O was higher than the uncertainty of measuring 0.5 ppmv of H_2S in dry air [37].

This variation on uncertainties concerning the H_2S concentrations – and therefore the removal efficiencies – is clearly visible on Figure 3A. Plotting only the removal efficiencies of H_2S obtained in dry condition (humidity level fixed at 100 ppmv of H_2O) as shown in Figure SI-1, Support Information, $T_{reactor}$ at 20 °C, 40 °C and 60 °C have shown similar behaviors as function of ozone concentration, indicating that removal of H_2S was not significantly affected by this parameter for the operating conditions applied. In addition, the increase of H_2S removal as function of ozone concentration has no longer presented a parabolic curve, showing only a slowdown with the ozone concentration. The falsely negative effect of $T_{reactor}$ according to ANOVA and the parabolic curve of fitting model may be the reflect of the model accuracy calculation since it is based on the repetition of the center of the domain and therefore, only one condition of humidity is evaluated.

In studies of gas ozonation, Tuggle [18] has also reported a lower impact of temperature on the removal efficiency of H_2S compared to DMDS: removal efficiency of H_2S has varied from 30% (at 38 °C) to 40% (at 125 °C) considering a residence time of 10 s and $[O_3]/[H_2S]$ molar ratio equal to 1. Otherwise for DMDS, for a $[O_3]$/[DMDS] molar ratio equal to 3 and a residence time

of 10 s, removal efficiency of DMDS has increased from 25% at 38 °C to 60% at 125 °C. DMS (the representative monosulfide studied by Tuggle [18]) has not been considerably affected by $T_{reactor}$ (65% and 70% removed at 38 °C and 125 °C respectively for a residence time equal to 10 s and $[O_3]/[DMS]$ equal to 2), which is in agreement to MES results, if we consider that monosulfide would react in a similar way with ozone.

3.3. Identification and quantification of oxidation products

3.3.1. Estimation of required parameters for SIFT/MS

The expected oxidation products of H_2S, MES and DMDS according to the literature are shown in Figure 5 [24,29,30]. In a first moment, we have considered the SO_2 and consequently, SO_3, were products of H_2S-O_3 reaction. Ozonation of MES would generate methyl ethyl sulfoxide (MESO) and sulfone ($MESO_2$), whereas the reaction between ozone and DMDS would probably produces methyl methanethiosulfinate (DMSOS), the isomers methyl methanesufonate ($DMSO_2S$) and dimethyl disulfoxide ($DM(SO)_2$), methylsulfinyl methyl sulfone ($DMSO_2SO$), dimethyl disulfone ($DM(SO_2)_2$) and methaneslfonic anhydride ($DM(SO_2)_2O$).

The required parameters for SIFT/MS quantification of SO_2 and SO_3 have been reported by Hera *et al* [41], which values are presented in Table 1. However, particularly for the expected oxidation products of MES and DMDS with ozone, their quantifications by SIFT/MS have not been stated, as far as we know. The only example of sulfoxide and sulfone present on LabSyft Compound Library® (release 1.6.2) were DMSO and $DMSO_2$, which characteristic product ions for H_3O^+ precursor ion were $(CH_3)_2SO.H^+$ *(79)* and $(CH_3)_2SO_2.H^+$ *(95)* and for NO^+ precursor ion, they were $(CH_3)_2SO^+$ *(78)* and $(CH_3)_2SO_2.NO^+$ *(124)*, respectively.

Therefore, in order to obtain the potential product ions for the expected oxidation products, we assumed that MESO would react with H_3O^+ and NO^+ precursor ions similarly to DMSO and $MESO_2$ to $DMSO_2$. As no information was found about the ionization of the oxidized disulfides compounds, we have considered that all potential oxidation products of DMDS would react with H_3O^+ by the standard H^+ transfer. For NO^+ precursor ion, a preliminary

analysis of the spectra was necessary since two ionization reactions may happen: by charge or NO^+ transfer. From Figure 6, we have identified that DMSOS, $DMSO_2SO$, $DM(SO_2)_2$ and $DM(SO_2)_2O$ would react with NO^+ by charge transfer, whereas the isomers $DMSO_2S$ and $DM(SO)_2$ by NO^+ transfer. The *m/z* = 126 (potentially related to $DMSO_2S$ and $DM(SO)_2$) has been identified on Figure 6. However, this peak was also quantified in the reactor inlet, being therefore neglected for the quantification of the isomers $DMSO_2S$ and $DM(SO)_2$. The assumed characteristic product ion for each expected product are in Table 1.

As described in Equation 1, the rate coefficient is also required to quantify an analyte by SIFT/MS. According to several studies in the literature [38,39,42,43], the rate coefficient of ionization reaction (k_I) could be estimated by the collision theory (kc) and calculated by method of Su [44,45] (Equation 5), which depends on the dipole moment (μ_D), polarizability (α) and molar mass of the neutral compound ($MM_{neutral}$), molar mass of the precursor ion (MM_{ion}), flow tube temperature (T_{ft}), elementary charge (e) and Boltzmann constant (k_b). When μ_D and α were not available on NIST [46,47], they were estimated by Avogadro® (version 1.0.1) and ACD/ChemSketch® (version 2018.1.1), respectively. The calculated kc are available in Table 1, which resulted close to experimental values, suggesting that estimation of k_I by kc should be valid.

The quantification of MES, DMDS and their expected oxidation products were carried out by NO^+ precursor ion, since it is less effected by the humidity level of the sample (compared to H_3O^+ that in presence of water vapor, generates water clusters $H_3O^+.(H_2O)_{n\ =\ 1,2,3}$) and therefore, the simple expression to calculate the compounds concentrations can be used (Equation 1) [48]. O_2^+ precursor also reacts with MES, DMDS and with their expected ozonation products; however, O_2^+ ionization reaction is less soft than H_3O^+ and NO^+, usually generating more than one characteristic product ion [38]. Since the O_2^+ spectra were much more complex than H_3O^+ and NO^+ spectra, the kinetics parameters were not calculated in this study.

$$kc = K_{CAP}\, 2\pi e \sqrt{\frac{\alpha}{\frac{MM_{ion} MM_{neutral}}{MM_{ion}+MM_{neutral}}}}, \text{with } K_{CAP} = \begin{cases} \frac{(x+0.5090)^2}{10.526} + 0.9754 \,;\, x < 2 \\ 0.4767x + 0.6200 \,;\, 2 < x < 3 \\ 0.5781x + 0.3165 \,;\, 3 < x < 35 \\ 0.6201x - 1.15 \,;\, 35 < x < 60 \\ 0.6347x - 2.029 \,;\, x \geq 60 \\ \text{with } x = \frac{1}{\sqrt{\frac{2\alpha k_b T_{ft}}{\mu_D}}} \end{cases} \quad (5)$$

3.3.2. Quantification of oxidation products

Even with the low removal efficiencies of MES and DMDS during this ozonation process, some of the expected oxidation products indicated in Figure 5 could be identified. From the characteristic product ions proposed in Table 1, $MESO_2$ and MESO, DMSOS and the isomers $DMSO_2S$ + $DM(SO)_2$ were detected in the NO^+ spectra of reactor outlet, as it is shown in Figure 6.

The molar yields of the oxidation products (φ_i) were obtained according to Equation 6 (taking as example the molar yield of MESO calculation), whose concentration ([i], with i = MESO) was calculated from the estimated parameters shown in Table 1. By applying Equation 6, the molar yield of MESO and $MESO_2$ (Figure 7A) and of DMSOS and the isomers $DMSO_2S$ + $DM(SO)_2$ (Figure 7B) were investigated in function of the removal efficiency of MES and DMDS, respectively.

$$\varphi_{MESO} = \frac{[MESO]}{[MES]_{in} - [MES]_{out}} \quad (6)$$

In case of MES, $MESO_2$ was identified as the primary product for the ozonation of MES, representing a molar yield equal to 70% in average, whereas MESO has resulted in a molar yield equal to 10%. In case of DMDS, DMSOS was present in a higher concentration than the isomers $DMSO_2S$ + $DM(SO)_2$, with a molar yield around 30% and 10%, respectively, for a removal efficiency of DMDS between 15% and 25%. The visible reduction of molar yield of DMSOS and $DMSO_2S$ + $DM(SO)_2$ with the increase of removal efficiency of DMDS in Figure 7B could be explained by the generation of SO_2 and SO_3. In Figure 8, the correlation of the DMDS consumption with $[SO_2]_{out}$ and $[SO_3]_{out}$ was evidenced, suggesting that ozone attacks

the sulfur-sulfur bond, generating SO_2, which may be the primary product of ozonation of DMDS. The additional peaks detected in Figure 6 at *m/z* ratio smaller than MES and DMDS could be related to potential by-products having a shorter carbon chain.

In summary, from the analysis of the primary products of MES and DMDS, we suggest that the gas phase ozonation of organic monosulfide and disulfide (in the operating conditions applied in this study) may happen by two different mechanisms: (*i*) monosulfides might be oxidized by an electrophilic attack of molecular ozone, as it is usually proposed in liquid phase, with a sequential oxygen-addition on sulfur molecule and (*ii*) the reaction of ozone with organic disulfide would be mainly led by the sulfur-sulfur bond scission.

Another important analysis could be extracted from Figure 8 regarding the ozonation of H_2S. In conditions where the consumption of RSCs was mainly represented by H_2S (experiments number 1 and 2 in Figure 8), the sum of the concentrations of SO_2 and SO_3 have not resulted in the quantity of H_2S consumed, implying that SO_2 may not be the only product of H_2S ozonation in the operating conditions applied in this study. Preliminary ozonation experiments carried out in presence of only H_2S (Figure SI-2, Support Information) have evidenced that the peak at *m/z* 81 in H_3O^+ spectra of the reactor outlet (Figure SI-3A, Support Information) and the peak at *m/z* 80 in O_2^+ spectra of the reactor outlet (Figure SI-3B, Support Information) were related to the reaction between H_2S and O_3, likely representing an by-product in addition to SO_2 and H_2O previously expected. However, as this compound could not be identified, its quantification by SIFT/MS was not possible.

Sulfuric acid, $DMSO_2SO$, $DM(SO_2)_2$ and $DM(SO_2)_2O$ proposed as potential products in Figure 5 were continuously followed during the experiments, however, their generation were negligible. Sulfuric acid represented less than 5% of all RSCs consumed, even in highest humidity levels and the sum of the molar yield of $DMSO_2SO$, $DM(SO_2)_2$ and $DM(SO_2)_2O$ represented less than 5% of DMDS variation.

As in most of experiments ozone was present in large excess, its consumption was insignificant (Figure 8). Nevertheless, for the experiments number 1 and 2 (Figure 8), a slight difference between the ozone concentration at the reactor inlet and outlet could be considered.

However, as the uncertainty of SIFT/MS quantification of ozone was higher at low concentration level, the consumption of ozone could not be measured.

4. Conclusion

The application of homogenous gas ozonation was studied with operating parameters similar to industrial conditions: short residence time (2 to 20 s); mild temperature (20 to 60 °C), ozone-RSCs molar ratio (0.8 to 20) and total RSCs concentration of 6.5 ppmv. Quite low removal efficiencies were obtained for MES and DMDS: maximum removal efficiencies up to 30% even when ozone was used in large excess (20 times the RSCs concentration). At the same time, H_2S has resulted in an interesting removal (up to 80%). In the studied experimental domain, ozone concentration has shown a slight positive impact for all three RSCs. In contrast, the other three operating parameters investigated (humidity level, reactor temperature and residence time) did not show significant influence on the removal efficiency of RSCs.

Besides the low efficiency for organic sulfides, the necessity of ozone at high excess must be highlighted as drawback of gas ozonation, since ozone emission must be avoided (considered an air pollution in ground-level [49]). A step of decomposition/destruction of ozone should therefore be planned. It would be relevant to couple the homogenous ozonation with another oxidative technique – such as reactive absorption, photocatalysis/photolysis or adsorption/catalysis – in order to enhance the overall removal efficiency of RSCs and overcome the drawbacks previously highlighted.

Primary products of ozone-RSCs reaction in gas phase were identified, suggesting that organic monosulfide and disulfide probably follow different reaction mechanisms. In case of monosulfide, sulfone was the primary product detected, indicating a reaction based on electrophilic attack of ozone with a sequential oxygen-addition on sulfur molecule. In case of disulfide, the mechanism would be mainly due to sulfur-sulfur bond scission, since SO_2 was the primary product detected. Nevertheless, complementary studies would be necessary in order to verify the hypothesis regarding the organic sulfides mechanism with ozone. Finally, SO_2 and H_2O may not be the only by-products for ozonation of H_2S, since additional peaks were detected in H_3O^+ and O_2^+ spectra of SIFT/MS analysis.

Acknowledgements

The authors gratefully acknowledge the financial support for the research by French National Agency for Research and Technology and Agro Innovation International (CIFRE 2015/1233). The authors thank Mr. Laurent Willain for his support and helpful advices.

References

[1] M. de Blas, M. Navazo, L. Alonso, G. Gangoiti, J.A. García, E.S. de Cámara, V. Valdenebro, E. García-Ruiz, N. García-Borreguero, Continuous measurement of atmospheric reduced sulphur compounds as key tracers between odour complaints and source apportionment, Environ. Monit. Assess. 189 (2017). doi:10.1007/s10661-017-5800-2.

[2] F. Carrera-Chapela, A. Donoso-Bravo, J.A. Souto, G. Ruiz-Filippi, Modeling the odor generation in WWTP: an integrated approach review, Water. Air. Soil Pollut. 225 (2014) 1–15. doi:10.1007/s11270-014-1932-y.

[3] A. Feilberg, D. Liu, A.P.S. Adamsen, M.J. Hansen, K.E.N. Jonassen, Odorant emissions from intensive pig production measured by online proton-transfer-reaction mass spectrometry, Environ. Sci. Technol. 44 (2010) 5894–5900. doi:10.1021/es100483s.

[4] J.R. Kastner, Q. Buquoi, R. Ganagavaram, K.C. Das, Catalytic ozonation of gaseous reduced sulfur compounds using wood fly ash, Environ. Sci. Technol. 39 (2005) 1835–1842. doi:10.1021/es0499492.

[5] R. Iranpour, H.H.J. Cox, M.A. Deshusses, E.D. Schroeder, Literature review of air pollution control biofilters and biotrickling filters for odor and volatile organic compound removal, Environ. Prog. 24 (2005) 254–267. doi:10.1002/ep.10077.

[6] D. Volckaert, P.M. Heynderickx, E. Fathi, H. Van Langenhove, SIFT-MS a novel tool for monitoring and evaluating a biofilter performance, Chem. Eng. J. 304 (2016) 98–105. doi:10.1016/j.cej.2016.04.138.

[7] A. Kerc, S.S. Olmez, Ozonation of odorous air in wastewater treatment plants, Ozone Sci. Eng. 32 (2010) 199–203. doi:10.1080/01919511003792102.

[8] E. Vega, M.J.; Martin, R. Gonzalez-Olmos, Integration of advanced oxidation processes at mild conditions in wet scrubbers for odourous sulphur compounds treatment, Chemosphere. 109 (2014) 113–119. doi:10.1016/j.chemosphere.2014.02.061.

[9] H. Yao, A. Feilberg, Characterisation of photocatalytic degradation of odorous compounds associated with livestock facilities by means of PTR-MS, Chem. Eng. J. 277 (2015) 341–351. doi:10.1016/j.cej.2015.04.094.

[10] Y. Zhang, K.R. Pagilla, Gas-phase ozone oxidation of hydrogen sulfide for odor treatment in water reclamation plants, Ozone Sci. Eng. 35 (2013) 390–398. doi:10.1080/01919512.2013.796861.

[11] X. Li, G. Zhang, H. Pan, Experimental study on ozone photolytic and photocatalytic degradation of H_2S using continuous flow mode, J. Hazard. Mater. 199–200 (2012) 255–261. doi:10.1016/j.jhazmat.2011.11.006.

[12] C. Meusinger, A.B. Bluhme, J.L. Ingemar, A. Feilberg, S. Christiansen, C. Andersen, M.S. Johnson, Treatment of reduced sulphur compounds and SO_2 by Gas Phase Advanced Oxidation, Chem. Eng. J. J. 307 (2017) 427–434. doi:10.1016/j.cej.2016.08.092.

[13] C.L. Hwang, N.H. Tai, Vapor phase oxidation of dimethyl sulfide with ozone over ion-exchanged zeolites, Appl. Catal. A Gen. 393 (2011) 251–256. doi:10.1016/j.apcata.2010.12.004.

[14] K. Skalska, S.S. Ledakowicz, R. Louwe, R.R. Szymczak, Nitrogen oxides pre-ozonation in flue gases from phosphate rock digestion, Chem. Eng. J. 318 (2017) 181–188. doi:10.1016/j.cej.2016.06.048.

[15] K. Skalska, J.S. Miller, S. Ledakowicz, Effectiveness of nitric oxide ozonation, S. Chem. Pap. 65 (2011) 193–197. doi:https://doi.org/10.2478/s11696-010-0082-y.

[16] Z. Wang, J. Zhou, Y. Zhu, W. Zhengcheng, J. Liu, K. Cen, Simultaneous removal of NO_x, SO_2 and Hg in nitrogen flow in a narrow reactor by ozone injection: Experimental results, Fuel Process. Technol. 88 (2017) 817–823. doi:https://doi.org/10.1016/j.fuproc.2007.04.001.

[17] L. Wei, J. Zhou, Z. Wang, K. Cen, Kinetic modeling of homogeneous low-temperature multi-pollutant oxidation by ozone, Ozone Sci. Eng. 29 (2007) 207–214. doi:10.1080/01919510701304046.

[18] M.L. Tuggle, Reactions of reduced sulfur compounds with ozone, University of Florida, 1971.

[19] R. Atkinson, D.L. Baulch, R.A. Cox, J.N. Crowley, R.F. Hampson, R.G. Hynes, M.E. Jenkin, M.J. Rossi, J. Troe, Evaluated kinetic and photochemical data for atmospheric chemistry: Volume I - gas phase reactions of O_x, HO_x, NO_x and SO_x species, Atmos. Chem. Phys. 4 (2004) 1461–1738. doi:10.5194/acp-4-1461-2004.

[20] R. Atkinson, W.P.L. Carter, Kinetics and mechanisms of the gas-phase reactions of ozone with organic compounds under atmospheric conditions, Chem. Rev. 84 (1984) 437–470. doi:10.1021/cr00063a002.

[21] F. Westley, Table of rate constants for gas phase chemical reactions of sulfur compounds (1971-1980), NIST (1982).

[22] K.H. Becker, M.A. Inocencio, U. Schurath, Reaction of ozone with hydrogen sul de and its organic derivatives, Int. J. Chem. Kinet. Conf. Symp. Chem. Kinet. Data Up. Low. Atmos. Warrenton, VA, USA, 15 Sep 1974. 7 (1975).

[23] M. Vahedpour, R. Baghary, F. Khalili, Prediction of mechanism and thermochemical properties of $O_3 + H_2S$ atmospheric reaction, J. Chem. (2013). doi:10.1155/2013/659682.

[24] S.H. Mousavipour, M. Mortazavi, O. Hematti, Multichannel RRKM-TST and direct-dynamics CVT study of the reaction of hydrogen sulfide with ozone, J. Phys. Chem. A. 117 (2013) 6744–6756. doi:10.1021/jp404738d.

[25] S. Glavas, S. Toby, Reaction between ozone and hydrogen sulfide, J. Phys. Chem. 79 (1975) 779–782. doi:10.1021/j100575a004.

[26] J.M. Hales, J.O. Wilkes, J.L. York, Some recent measurements of H_2S oxidation rates and their implications to atmospheric chemistry, Tellus. 26 (1974) 277–283. doi:10.3402/tellusa.v26i1-2.9795.

[27] S.T. Oyama, Chemical and Catalytic Properties of Ozone, Catal. Rev. 42 (2000) 279–322. doi:10.1081/CR-100100263.

[28] W. Du, Lin; Xu, Yongfu; Ge; Jia, Long; Yao, Li; Wang, L. Du, Y. Xu, M. Ge, L. Jia, L. Yao, W. Wang, Rate constant of the gas phase reaction of dimethyl sulfide (CH_3SCH_3) with ozone, Chem. Phys. Lett. 436 (2007) 36–40. doi:10.1016/j.cplett.2007.01.025.

[29] P.S. Bailey, The reactions of ozone with organic compounds, Chem. Rev. 58 (1958) 925–1010. doi:10.1021/cr50023a005.

[30] D. Barnard, Oxidation of organic sulphides. Part IX. The reaction of ozone with organic sulphur compouds, J. Chem. Soc. (1957) 4547–4555.

[31] I.B. Douglass, Some chemical aspects of kraft odor control, J. Air Pollut. Control Assoc. 18

(1968) 541–545. doi:10.1080/00022470.1968.10469169.

[32] R.I. Martinez, J.T. Herron, Stopped-flow study of the gas-phase reaction of ozone with organic sulfides: dimethyl sulfide, Int. J. Chem. Kinet. 10 (1978) 433–452.

[33] R.J. Glinski, D.A. Dixon, Chemiluminescent reactions of ozone with dimethyl sulfoxide and dimethyl disulfide. Formation of electronically excited sulfur dioxide, J. Phys. Chem. 89 (1985) 33–38. doi:10.1021/j100247a010.

[34] E.C. Sivret, B. Wang, G. Parcsi, R.M. Stuetz, Prioritisation of odorants emitted from sewers using odour activity values, Water Res. 88 (2016) 308–321. doi:10.1016/j.watres.2015.10.020.

[35] X. Yang, W. Zhu, J.A. Koziel, L. Cai, W.S. Jenks, Y. Laor, J.H. van Leeuwen, S.J. Hoff, Improved quantification of livestock associated odorous volatile organic compounds in a standard flow-through system using solid-phase microextraction and gas chromatography-mass spectrometry, J. Chromatogr. A. 1414 (2015) 31–40. doi:10.1016/j.chroma.2015.08.034.

[36] F. Lestremau, V. Desauziers, J.C. Roux, J.L. Fanlo, Development of a quantification method for the analysis of malodorous sulphur compounds in gaseous industrial effluents by solid-phase microextraction and gas chromatography-pulsed flame photometric detection, J. Chromatogr. A. 999 (2003) 71–80. doi:10.1016/S0021-9673(03)00328-5.

[37] L. Vitola Pasetto, R. Richard, J.-S. Pic, M.-H. Manero, F. Violleau, V. Simon, Hydrogen sulphide quantification by SIFT/MS: highlighting the influence of gas moisture, Int. J. Environ. Anal. Chem. (2019). doi:https://doi.org/10.1080/03067319.2019.1650919.

[38] D. Smith, P. Spanel, Selected Ion Flow Tube Mass Spectrometry (SIFT-MS) for on-line trace gas analysis, Mass Spectrom. Rev. 24 (2005) 661–700. doi:10.1002/mas.20033.

[39] G.J. Francis, D.B. Milligan, M.J. McEwan, Detection and quantification of chemical warfare agent precursors and surrogates by selected ion flow tube mass spectrometry, Anal. Chem. 81 (2009) 8892–8899. doi:10.1021/ac901486c.

[40] S.L.C. Ferreira, W.N.L. Dos Santos, C.M. Quintella, B.B. Neto, J.M. Bosque-Sendra, Doehlert matrix: A chemometric tool for analytical chemistry - Review, Talanta. 63 (2004) 1061–1067. doi:10.1016/j.talanta.2004.01.015.

[41] D. Hera, V. Langford, M. McEwan, T. McKellar, D. Milligan, Negative reagent ions for real time detection using SIFT-MS, Environments. 4 (2017) 16. doi:10.3390/environments4010016.

[42] B. R'Mili, B. Temime-roussel, A. Monod, H. Wortham, R.S. Strekowski, Quantification of the gas phase methyl iodide using O_2^+ as the reagent ion in the PTR-ToF-MS technique, Int. J. Mass Spectrom. 431 (2018) 43–49. doi:10.1016/j.ijms.2018.06.003.

[43] J. Zhao, R. Zhang, Proton transfer reaction rate constants between hydronium ion (H_3O^+) and volatile organic compounds, Atmos. Environ. 38 (2004) 2177–2185. doi:10.1016/j.atmosenv.2004.01.019.

[44] T. Su, Erratum : Trajectory calculations of ion- polar molecule capture rate constants at, J. Chem. Phys. 89 (1988) 5355. doi:10.1063/1.455750.

[45] T. Su, W.J. Chesnavich, Parametrization of the ion – polar molecule collision rate constant by trajectory calculations, J. Chem. Phys. 76 (1982) 5183–5185. doi:10.1063/1.442828.

[46] NIST - computational chemistry comparison and benchmark dataBase - experimental dipoles. https://cccbdb.nist.gov/diplistx.asp, 2019 (accessed March 1, 2019).

[47] NIST - computational chemistry comparison and benchmark dataBase - experimental polarizabilites. https://cccbdb.nist.gov/pollistx.asp, 2019 (accessed March 1, 2019).

[48] P. Spanel, D. Smith, Influence of water vapour on selected ion flow tube mass spectrometric

analyses of trace gases in humid air and breath, Rapid Commun. Mass Spectrom. 14 (2000) 1898–1906.

[49] World Health Organization, Air quality guidelines for particulate matter, ozone, nitrogen dioxide and sulfur dioxide - Global update, 2005.

[50] L. Vitola Pasetto, R. Richard, J.-S. Pic, M.-H. Manero, F. Violleau, V. Simon, Ozone quantification by Selected Ion Flow Tube Mass Spectrometry: influence of humidity and manufacturing gas of ozone generator, Anal. Chem. *in press* (2019).

Figure and Tables

Table 1. Required parameters for quantification by SIFT/MS of reagents (RSCs and ozone) and expected oxidation products.

Compound	CAS number	μ_D (De)	α (A^3)	H_3O^+		NO^+		O_2^-		NO_2^-	
				product ion *(m/z)*	k_I[a] [kc][a]	product ion *(m/z)*	k_I[a] [kc][a]	product ion *(m/z)*	k_I[a]	product ion *(m/z)*	k_I[a]
Reagents											
O_3	10028-15-6	-	-	-	-	-	-	-	-	NO_3^- *(-62)*	0.11[g]
H_2S	7783-06-4	0.97[b]	3.631[c]	H_3S^+ *(35)*	1.6[b] [2]	-	-	-	-	-	-
MES	624-89-5	1.56[b]	9.49[c]	$C_2H_5SCH_3.H^+$ *(77)*	2.4[e] [2.6]	$C_2H_5SCH_3^+$ *(76)*	2.1[e] [2.2]	-	-	-	-
DMDS	624-92-0	1.985[b]	10.82[c]	$(CH_3S)_2.H^+$ *(95)*	2.6[e] [2.7]	$(CH_3S)_2^+$ *(94)*	2.4[e] [2.3]	-	-	-	-
Expected products											
MESO	1669-98-3	3.779	9.83	$C_2H_5SOCH_3.H^+$ *(93)*	- [3.3]	$C_2H_5SOCH_3^+$ *(92)*	- [2.7]	-	-	-	-
$MESO_2$	594-43-4	4.176	9.8	$C_2H_5SO_2CH_3.H^+$ *(109)*	- [3.3]	$C_2H_5SO_2CH_3.NO^+$ *(138)*	- [2.8]	-	-	-	-
DMSOS	13882-12-7	2.072	11.16	$(CH_3)_2SOS.H^+$ *(111)*	- [2.8]	$(CH_3)_2SOS^+$ *(110)*	- [2.3]	-	-	-	-
$DMSO_2S$	2949-92-0	2.369	11.15	$(CH_3)_2SO_2S.H^+$ *(127)*	- [2.8]	$(CH_3)_2SO_2S.NO^+$ *(156)*	- [2.3]	-	-	-	-
$DM(SO)_2$	98984-65-7	0.685	11.51	$(CH_3SO)_2.H^+$ *(127)*	- [2.3]	$(CH_3SO)_2.NO^+$ *(156)*	- [1.9]	-	-	-	-
$DMSO_2SO$	14128-56-4	1.576	11.49	$(CH_3)_2SO_2SO.H^+$ *(143)*	- [2.6]	$(CH_3)_2SO_2SO^+$ *(142)*	- [2.1]	-	-	-	-
$DM(SO_2)_2$	10383-49-0	0.041	11.47	$(CH_3SO_2)_2.H^+$ *(159)*	- [2.0]	$(CH_3SO_2)_2^+$ *(158)*	- [1.6]	-	-	-	-
$DM(SO_2)_2O$	7143-01-3	5.844	12.16	$(CH_3SO_2)_2O.H^+$ *(175)*	- [3.7]	$(CH_3SO_2)_2O^+$ *(174)*	- [3.1]	-	-	-	-
H_2SO_4	7664-93-9	-	-	$H_3SO_4^+$ *(99)*	0.7[e]	-	-	-	-	-	-
SO_2	7446-09-5	-	-	-	-	-	-	SO_2^- *(-64)*	1.9[d]	-	-
SO_3	7446-11-9	-	-	-	-	-	-	SO_3^- *(-80)*	1.5[f]	-	-

a. 10^{-9} cm^3 $molecule^{-1}$ s^{-1}.
b. Experimental values obtained from NIST [46].
c. Experimental values obtained from NIST [47].
d. Value of rate coefficient at dry condition. Rate coefficient of H_2S with H_3O^+ requires correction according to the humidity level [37].
e. Kinetics parameters obtained from LabSyft Compound Library® (release 1.6.2).
f. Kinetics parameters obtained from Hera *et al* [41].
g. Kinetics parameters obtained from Vitola Pasetto *et al* [50].

Table 2. Range of humidity level, inlet ozone concentration and reactor temperature applied in the experimental design with $[H_2S]_{in}$ = 0.46 ± 0.08 ppmv; $[MES]_{in}$ = 1.8 ± 0.2 ppmv; $[DMDS]_{in}$ = 4.0 ± 0.4 ppmv and t_{RES} = 2s.

Factors	U_1	U_2	U_3
	$[H_2O]$ (ppmv)	$[O_3]_{in}$ (ppmv)	$T_{reactor}$ (°C)
Minimum	100	5	20
Maximum	40000	100	60

Table 3. Analysis of variance (ANOVA) for removal efficiencies of H_2S, MES and DMDS (P-value < 0.005 are in bold).

Model				
		Y_{H2S}	Y_{MES}	Y_{DMDS}
	R^2	0.9528	0.9912	0.9771
	P-value	**0.001**	**0**	**0**
Coefficient		**P-value**		
Constant	a_0	**0**	**0**	**0**
$[H_2O]$	a_1	0.366	0.549	0.105
$[O_3]_{in}$	a_2	**0**	**0**	**0**
$T_{reactor}$	a_3	**0**	0.996	**0**
$[H_2O] \times [H_2O]$	a_{11}	0.012	0.706	0.203
$[O_3]_{in} \times [O_3]_{in}$	a_{22}	**0.004**	**0.004**	0.629
$T_{reactor} \times T_{reactor}$	a_{33}	0.535	0.006	**0.002**
$[H_2O] \times [O_3]_{in}$	a_{12}	0.981	0.714	0.591
$[H_2O] \times T_{reactor}$	a_{13}	0.892	0.073	0.294
$[O_3]_{in} \times T_{reactor}$	a_{23}	0.648	0.659	0.17

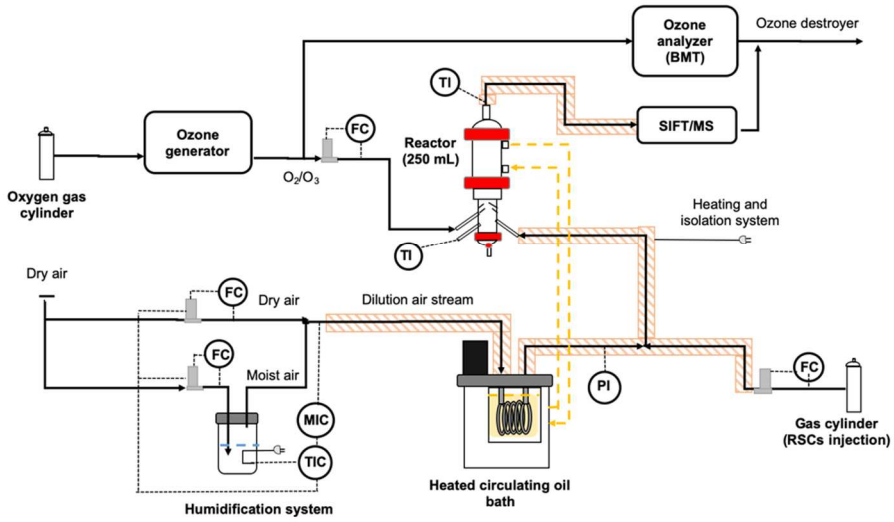

Figure 1. Experimental set-up.

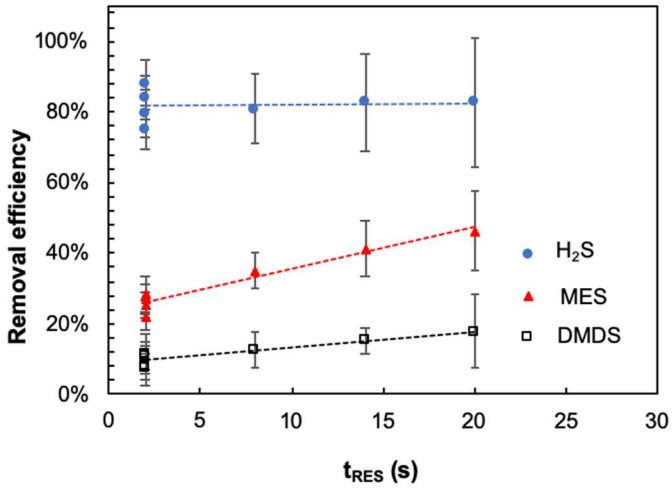

Figure 2. Removal efficiency of H_2S, MES and DMDS as function of t_{RES} for $[H_2S]_{in}$ = 0.46 ± 0.08 ppmv; $[MES]_{in}$ = 1.8 ± 0.2 ppmv; $[DMDS]_{in}$ = 4.0 ± 0.4 ppmv, $[O_3]_{in}$ = 100 ppmv and $T_{reactor}$ = 20 °C.

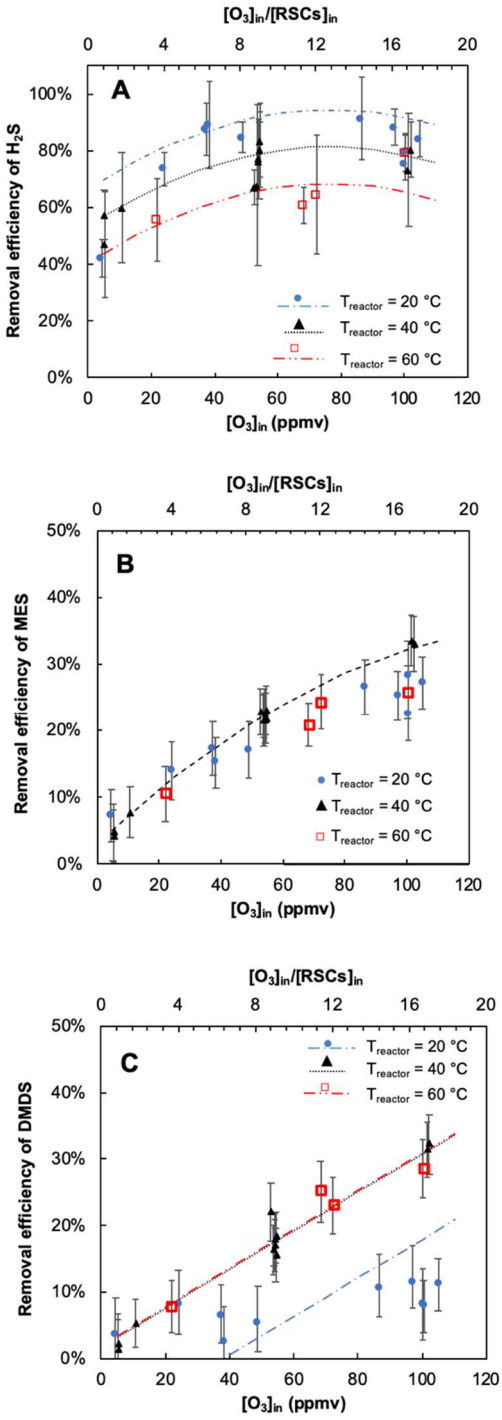

*Figure 3. Removal efficiency of H_2S (**A**), MES (**B**) and DMDS (**C**) as function of the inlet ozone concentration under different $T_{reactor}$, for $[H_2S]_{in}$ = 0.46 ± 0.08 ppmv; $[MES]_{in}$ = 1.8 ± 0.2 ppmv; $[DMDS]_{in}$ = 4.0 ± 0.4 ppmv and t_{RES} = 2 s.*

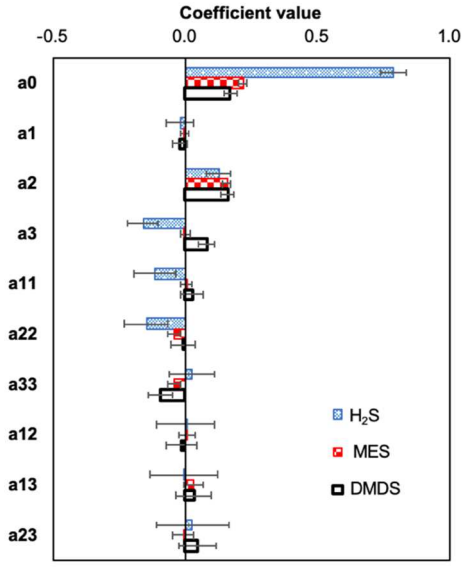

Figure 4. Coefficient values of Doehlert models for removal efficiencies of H_2S, MES and DMDS obtained considering a confidential interval of 95%.

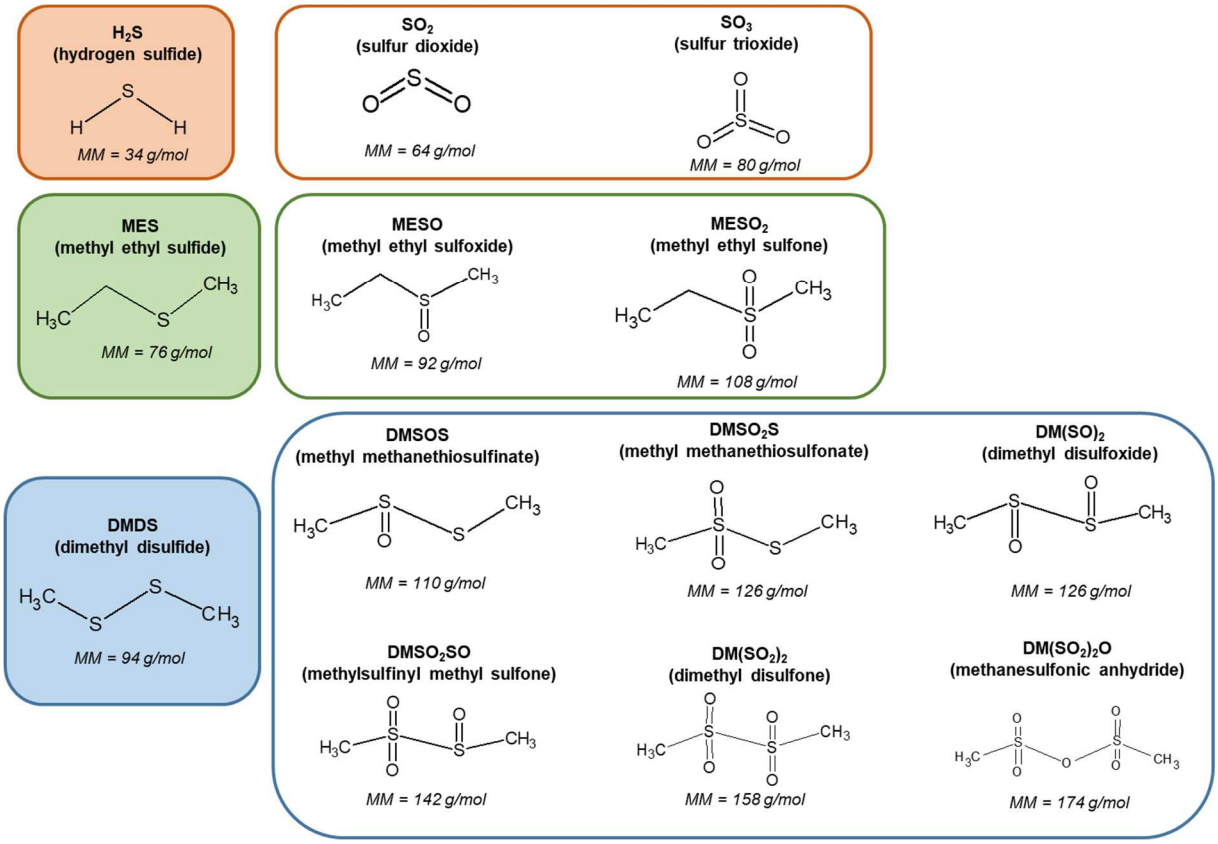

Figure 5. RSCs and their expected oxidation products according to the reactional mechanism proposed in the literature [24,29,30].

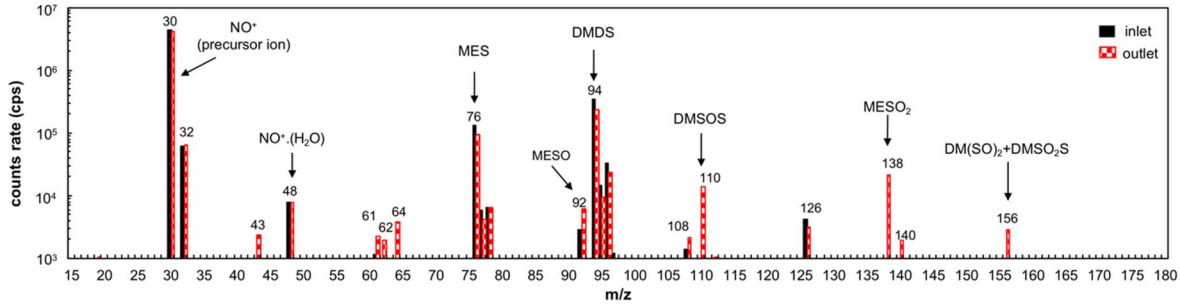

Figure 6. Comparison of NO^+ spectra at the reactor inlet with the reactor outlet for $[H_2S]_{in}$ = 0.46 ± 0.08 ppmv; $[MES]_{in}$ = 1.8 ± 0.2 ppmv; $[DMDS]_{in}$ = 4.0 ± 0.4 ppmv, $[O_3]_{in}$ = 100 ppmv, t_{RES} = 2 s and $T_{reactor}$ = 60 °C.

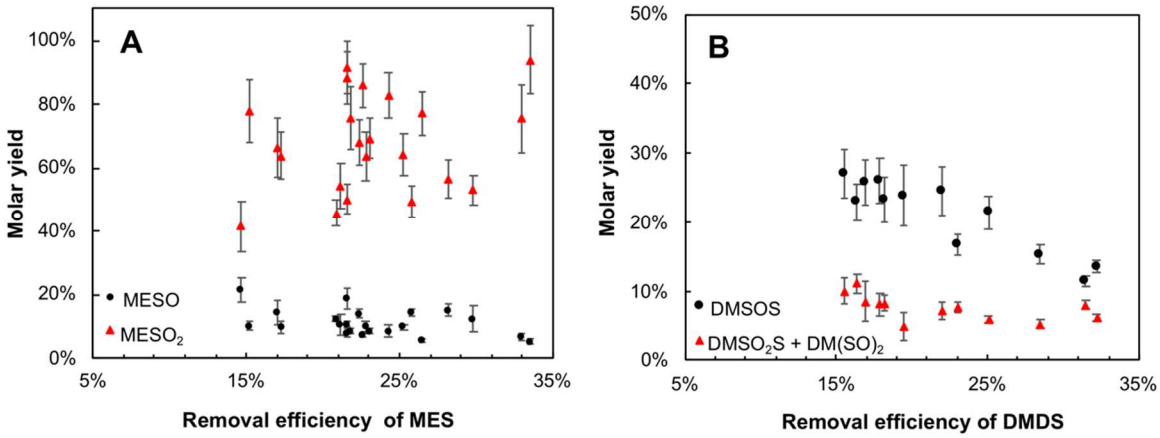

*Figure 7. **A**) Molar yield of the MESO and $MESO_2$ as function of removal efficiency of MES. **B**) Molar yield of DMSOS and the sum of the isomers $DMSO_2S$ and $DM(SO)_2$ as function of removal efficiency of DMDS. Only the experiments with removal efficiency superior to 15 % were considered due to the extremely high uncertainty at the low range (< 15%).*

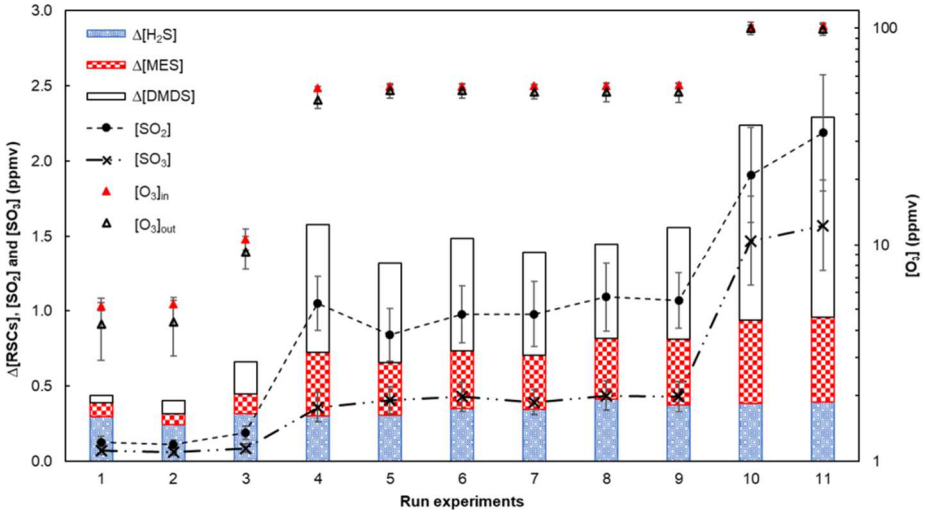

Figure 8. Comparison of RSCs consumed with the concentration of SO_2 and SO_3 measured at the reactor outlet and with the ozone concentration at the reactor inlet and outlet. Experiments carried out with t_{RES} of 2 s and $T_{reactor}$ at 40 °C.

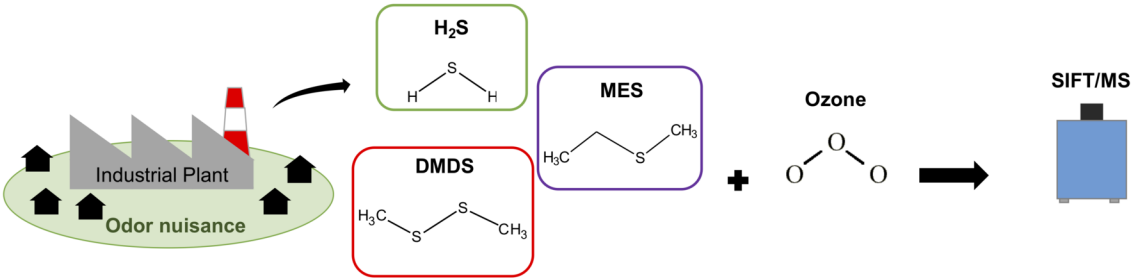

Process investigation

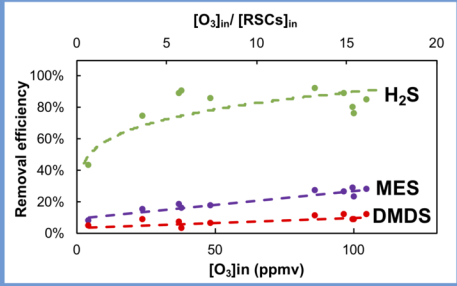

End products quantification